A data-driven solver scheme for inelastic problems

Erik Prume, Laurent Stainier, Michael Ortiz, Stefanie Reese

Received: 7 October 2022 | Accepted: 13 December 2022

DOI: 10.1002/pamm.202200153

A data-driven solver scheme for inelastic problems

Erik Prume[1,*], **Laurent Stainier**[2], **Michael Ortiz**[3,4], and **Stefanie Reese**[1]

[1] Institute of Applied Mechanics, RWTH Aachen University, Mies-van-der-Rohe-Str. 1, 52074 Aachen, Germany
[2] Institute of Civil and Mechanical Engineering, Ecole Centrale Nantes, 1 rue de la Noe, 44321 Nantes, France
[3] Hausdorff Center for Mathematics, Universität Bonn, Endenicher Allee 60, 53115 Bonn, Germany
[4] Division of Engineering and Applied Science, California Institute of Technology, 1200 E. California Blvd., Pasadena, CA 91125, USA

We review the data-driven computing paradigm for inelastic problems. We extend an efficient graph search algorithm for the data search by thermodynamic constraints and a rate independent history parametrization based on the mechanical work increment. In addition, we propose a strategy how to use commercial solvers in the framework. Finally, we demonstrate the proposed method with a numerical example featuring 2-d continuum plasticity.

1 Introduction

1.1 Data-driven computing paradigm

This work is based on the data-driven computing paradigm proposed in [1]. Therein, the solution of mechanical boundary value problems is formulated directly in the stress and strain data without introducing a constitutive model. The motivation of this approach is to minimize the model uncertainties introduced by a classical constitutive modeling step, while simultaneously preserving physical laws, such as equilibrium and compatibility conditions, which are known precisely without any knowledge uncertainties. Model uncertainties occur due to the non-unique choice of possible functionals, an often difficult calibration procedure or uncertainties regarding the range of usage of the model. In case of an incremental data acquisition the process of modeling and calibration often leads to an open-ended process.

We briefly summarize the framework. The mechanical system with m material points is characterized by the strain field $\epsilon = \{\epsilon_e \in \mathbb{R}^d,\ e = 1, \dots, m\}$ and the stress field $\sigma = \{\sigma_e \in \mathbb{R}^d,\ e = 1, \dots, m\}$. The system state may be viewed as a point $z = \{z_e\}_{e=1}^m$ in the global phase space $Z = \mathbb{R}^{md \times md}$. The global phase space is equipped with a suitable norm

$$\|z\|^2 = \|(\epsilon, \sigma)\|^2 = \sum_{e=1}^{m} w_e \Big(\mathbb{C}_e \epsilon_e \cdot \epsilon_e + \mathbb{C}_e^{-1} \sigma_e \cdot \sigma_e \Big), \tag{1}$$

which defines a measure of distance with the metric coefficients $\mathbb{C}_e$. Hereby, w_e denotes the volume of material point e.

In addition, we define the global data set $D = D_1 \times \cdots \times D_m$ as the collection of local data sets D_e which consists of experimental data. A global data point $y_i \in D$ is then one possible assignment of local data points $y_{e,i}$ to each material point.

The physical constraints are given by equilibrium and compatibility

$$\sum_{e=1}^{m} w_e B_e^T \sigma_e = f, \tag{2a}$$

$$\epsilon_e = B_e u, \quad e = 1, \dots m, \tag{2b}$$

whereby B_e is the gradient operator relating the displacement field u to the strain field in material point e, given suitable boundary conditions for u and the force field f.

These constraints are then encoded by the constraint set $E \subset Z$ which contains all states $z \in Z$ satisfying Eqs. 2. The so-called *min-dist* solution is then defined by the data point closest to the constraint set:

$$y_{\mathrm{MD}} = \min_{y_i \in D} \|y_i - z_i\|^2 \tag{3}$$

with the closest point projection

$$z_i = P_E(y_i) = \min_{z \in E} \|z - y_i\|^2 \tag{4}$$

* Corresponding author: e-mail erik.prume@ifam.rwth-aachen.de

onto the constraint set E. As presented in [1], the closest point projection is solved by two linear, decoupled systems of equations

$$\left(\sum_{e=1}^{m} w_e B_e^T \mathbb{C}_e B_e\right) u = \sum_{e=1}^{m} w_e B_e^T \mathbb{C}_e \epsilon'_{e,i} \tag{5a}$$

$$\left(\sum_{e=1}^{m} w_e B_e^T \mathbb{C}_e B_e\right) \eta = f - \sum_{e=1}^{m} w_e B_e^T \sigma'_{e,i} \tag{5b}$$

for a given data point $y_i = \{\epsilon'_{e,i}, \sigma'_{e,i}\}_{e=1}^m$. The closest compatible state $z_i = \{\epsilon_{e,i}, \sigma_{e,i}\}_{e=1}^m$ is then given by

$$\epsilon_{e,i} = B_e u \tag{6a}$$

$$\sigma_{e,i} = \sigma'_{e,i} + \mathbb{C}_e B_e \eta. \tag{6b}$$

It should be noted that a direct evaluation of Eq. (3) is of combinatorial complexity since the number of possible assignments of local data points to material points (size of D) grows exponentially with the number of material points. To overcome this, [1] proposed a heuristic solver scheme which iterates between the projection operation defined by Eqs. (5)-(6) and a nearest neighbor (NN) search which finds the optimal local data point

$$\arg \min_{y_{e,i} \in D_e} \|y_{e,i} - z_e\|^2 \tag{7}$$

with respect to the current state z_e. Since the overall performance depends crucially on an efficient NN search, [2] investigated various data structures and approximate NN search techniques for elastic problems. While the k-means tree seems the most appropriate data structure for the elastic case, the kNN-graph shows interesting properties for incremental problems, as elaborated in Section 2. As also noted in [3, 4], the heuristic solver scheme does not necessarily find the global minimizer.

1.2 Extension to inelasticity

In [5], the framework was extended to inelastic problems. The principial idea was to restrict the data set to the admissible data given the deformation history, for which several parametrization techniques were presented. One particular choice of such a parametrization is

$$D_{e,k+1} = \{y_{e,i,k+1} \in D_e : y_{e,i,k}\} \tag{8}$$

whereby the data is labeled by time markers for time steps k. The associated solver then computes the optimal (i.e. closest to $E_{k=1}$) data point $y_{i,k+1} \in D_{k+1}$ while simultaneously minimizing the distance between its "history point" $y_{i,k} \in D_k$ and the compatible state from the last time step z_k. It should be noted that this parametrization captures only the short-term memory and is not sufficient for data involving long-term effects such as isotropic hardening. In addition, the parametrization Eq. (8) requires that the (pseudo) time discretization in the data has to match the time discretization of the evolving constraint set E_{k+1}. This makes in particular computations for rate-independent plasticity difficult, since it imposes an artificial constraint on the rate of deformation. This issue will be further addressed in Section 2. In this work, we make in addition use of the second law of thermodynamics, as was proposed first by [6] in the present context. Therein, the availability of thermodynamic quantities such as free energy or dissipation was motivated by the raise of high-fidelity micro-mechanical models used for data acquisition. In the discretized form, the dissipation inequality reads

$$\frac{1}{2}(\sigma'_{e,i,k+1} + \sigma'_{e,i,k}) \cdot (\epsilon'_{e,i,k+1} - \epsilon'_{e,i,k}) - (\psi'_{e,i,k+1} - \psi'_{e,i,k}) \geq 0 \tag{9}$$

which restricts the attainable data points y_{k+1} to those satisfying the second law of thermodynamics. We note, that the linear approximation of the mechanical work increment in Eq. (9) restricts the time step size in the regime of non-linear material behavior.

The rest of the paper is structured as follows. In Section 2, we propose an efficient data search method tailored around Eq. (9) using a deformation rate independent history parametrization. In Section 3 we discuss a strategy to make non-intrusive use of commercial finite element solver for the presented data-driven framework. In Section 4 we present a numerical example featuring a 2-d continuum boundary value problem with rate-independent plasticity using the proposed methods. We conclude the work and give an outlook for future work in Section 5.

2 Graph search

In [2], the performance of the k nearest neighbor (kNN) graph data structure was investigated for the nearest neighbor search for elastic problems defined in Eq. (7). Here, we extend the graph search to inelastic problems under constraint Eq. (9). At the

initialization of the kNN graph, each data point $y_{e,i}$ stores its k nearest neighbors $\mathcal{N}_i \subset D_e$. For elastic problems, the search starts at an initial data point $y_{e,i}$ and proceeds with optimal moves

$$y_{e,i} \leftarrow \arg \min_{y_{e,j} \in \mathcal{N}_i} \|y_{e,j} - z_e\|^2 \tag{10}$$

until $\|y_{e,j} - z_e\|^2 \geq \|y_{e,i} - z_e\|^2$ for all $y_{e,j} \in \mathcal{N}_i$. Since the search is performed only locally, it is not guaranteed to find the true nearest neighbor, or global minimum of Eq. (7). On the other side, this local search scheme is in particular efficient when an appropriate starting point can be provided, which is the case for inelastic problems. Due to its incremental nature the solution of the last time step can be used as an appropriate starting point, thus accelerating the kNN graph search.

We proceed by including the dissipation inequality by restricting $\mathcal{N}_i$ only to data points which allow thermodynamically consistent moves, that is

$$\mathcal{N}_i^{\mathrm{TC}} = \left\{ y_{e,j} \in \mathcal{N}_i : \frac{1}{2}(\sigma'_{e,j} + \sigma'_{e,i}) \cdot (\epsilon'_{e,j} - \epsilon'_{e,i}) - (\psi'_{e,j} - \psi'_{e,i}) \geq 0 \right\}. \tag{11}$$

One should note the subtle difference to Eq. (9). While in Eq. (9) the constraint is imposed on the whole time step, by Eq. (11) has imposes the constraint on each move. We argue that, if each move within the graph is thermodynamical consistent, the constraint is also fulfilled for the whole time step. Imposing the constraint by Eq. (11) by has the advantage that the admissible moves can be pre-computed offline. In addition, since only small, local moves are subject to the constraint, the linear approximation of the mechanical work holds also for non-linear time steps. However, restriction (11) alone is not sufficient. We complement the parametrization by a constraint on the deformation history. In particular, we propose a parametrization based on the mechanical work increment which is independent of the rate, thus avoiding the problems of parametrization (8) as discussed above. In [5], a history variable is re-interpreted as a variable which stores partial information of the stress strain history. Keeping this in mind, we define the history variable

$$q_{e,i} = \sum_{k=1}^{k_i} \frac{1}{2}(\sigma'_{e,i,k} + \sigma'_{e,i,k-1}) \cdot (\epsilon'_{e,i,k} - \epsilon'_{e,i,k-1}) \tag{12}$$

as the total mechanical work to reach data point $y_{e,i}$. Hereby, we have assumed that the ordering of the data path of length k_i to point $y_{e,i}$ and $y_{e,i,0} = (0, 0)$ is known. With this at hand, we define the subset

$$\mathcal{N}_i^{\mathrm{WC}} = \left\{ y_{e,j} \in \mathcal{N}_i : \left| \frac{1}{2}(\sigma'_{e,j} + \sigma'_{e,i}) \cdot (\epsilon'_{e,j} - \epsilon'_{e,i}) - (q_{e,j} - q_{e,i}) \right| \leq \mathrm{TOL} \right\} \tag{13}$$

as all data points within the graph neighbors which are consistent with the measured work increment. Finally, we apply both constraints (11, 13)

$$\mathcal{N}_i^{\mathrm{C}} = \mathcal{N}_i^{\mathrm{TC}} \cap \mathcal{N}_i^{\mathrm{WC}} \tag{14}$$

which defines the admissible graph neighborhood, as also illustrated in Fig. (1). Finally, these constraints define the graph structure used for the nearest neighbor search scheme as given in Eq. (10).

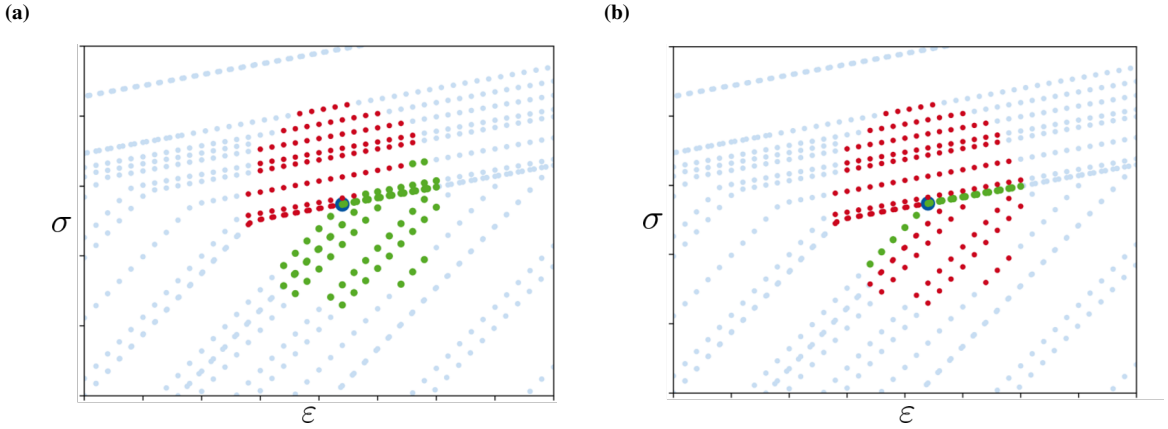

Fig. 1: Visualization of the constraints on a 1-d plasticity data set with isotropic hardening. a) Graph neighborhood after application of the dissipation inequality constraint (11). Green data points denote $\mathcal{N}_i^{\mathrm{TC}}$. b) Graph neighborhood after application of both constraints (11,13). Green data points denote $\mathcal{N}_i^{\mathrm{TC}} \cap \mathcal{N}_i^{\mathrm{WC}}$. Red data points denote the non-admissible neighborhood around blue center points $y_{e,i}$.

3 Using commercial solvers

An important aspect for the further application of the data-driven computing paradigm [1] is the usability of commercial finite element codes for the equilibrium projection (5). To the authors knowledge, this was not explicitly addressed in the literature so far. However, a few aspects have to be carefully considered. Since no functional relationship between stresses and strains is assumed, the number of degrees of freedom is doubled by introducing the Lagrange multipliers η. Even though it is possible to implement a data-driven solver with user-elements featuring additional degrees of freedom and included data sets, we argue that this approach has besides technical difficulties also conceptual drawbacks.

In particular, we emphasize the modular nature of the present framework. First, the two systems of equations (5) are decoupled and linear, even for non-linear material behavior. Therefore, only a single decomposition has to be performed. Secondly, the data search is decoupled from the equilibrium projection. In particular, concepts for history parametrizations for inelastic material behavior concern only the data search, and are not involved in equilibrium and compatibility. Lastly, the data storage and data acquisition are decoupled from the solver process. This has not only the advantage that large data sets have not to be loaded by the FE-solver, but also simplifies the collaborative work between structural analysts and material data specialists from experimental science or micro-scale modeling. Decoupling leads to a *query*-based usage of the FE-solver, complementing the query-based usage of the data search. Hereby, a data point (the query) is processed by the two linear elastic problems to compute the closest compatible state (the return value). This concept is also illustrated in Fig. (2).

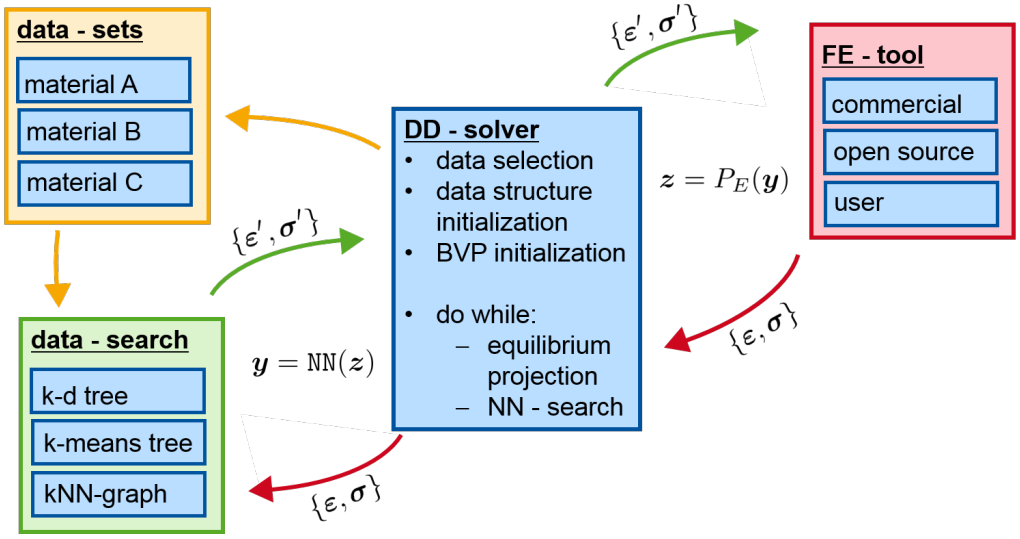

Fig. 2: Concept map for the modular parts of the data-driven computing paradigm. Green arrows are data point queries/return values, red arrows are compatible state queries/return values.

However, a suitable interface to the FE-solver is required. The global stiffness matrix can be assembled by linear elastic standard elements with the metric coefficients $\mathbb{C}_e$ as stiffness. User-element implementations can thus be avoided. However, two boundary value problems has to be set up to consider the different boundary conditions of the sub-problems (5a) and (5b). The key observation for the interface is that the to be projected data points can be included non-intrusively as an initial stress field. For systems (5a) and (5b) we set $\{\mathbb{C}_e \epsilon'_{e,i}\}_{e=1}^m$ and $\{\sigma'_{e,i}\}_{e=1}^m$ as initial stress field, respectively. Such an interface was developed for the commercial FE software ABAQUS using its .odb format for data exchange, demonstrated in the Section 4. However, the performance suffers currently due to the repeated calls to the software without dedicated interface.

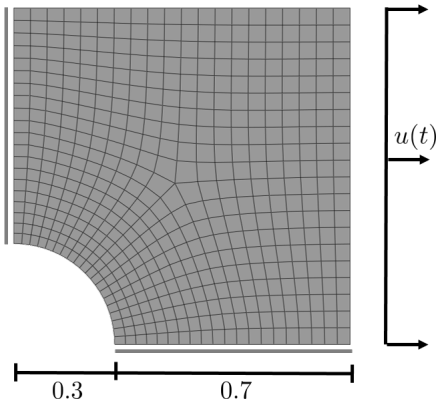

Fig. 3 Boundary value problem with a prescribed, non-proportional displacement $u(t)$.

Independent from this, we belief that the presented concept gives a guideline for developing and using software for data-driven computations.

4 Results

In order to verify the proposed method, we consider the 2-d continuum plate with a hole example shown in Fig. 3. The prescribed displacement $u(t)$ is increased to 0.1 and then decreased back to 0, resulting in residual stresses due to the plastic material behavior. For verification purposes, the material data was obtained from the reference solution using a plane stress, isotropic hardening von Mises plasticity model with elastic material parameters $E = 1000$ MPa, $\nu = 0.3$ and yield stress $\sigma_y = 50$ MPa. The data set contains in total 400000 data points, with metric coefficients $\mathbb{C}_e$ chosen to the elastic stiffness matrix. The mesh consists of 500 elements with 4 integration points, that is, $m = 2000$. In Fig. 4 the contour plots of the von Mises residual stress after unloading are shown for the reference and data-driven solution. The good agreement indicates that the proposed method captures successfully the inelastic behavior. Hereby, we have chosen the number of graph neighbors $k = 500$.

Finally, we investigate the influence of the number of graph neighbors on accuracy and CPU time in Fig. 5. In Fig. 5b) the error, computed by the norm defined in Eq. (1), in the last time step is shown in dependency on the number of graph

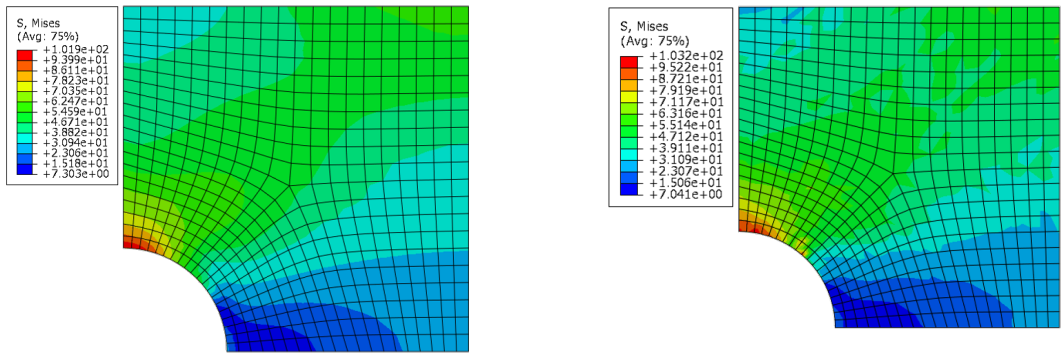

(a) **(b)**

Fig. 4: Von Mises residual stress after unloading. a) Reference solution. b) Data-driven solution using graph search using ABAQUS for equilibrium projections.

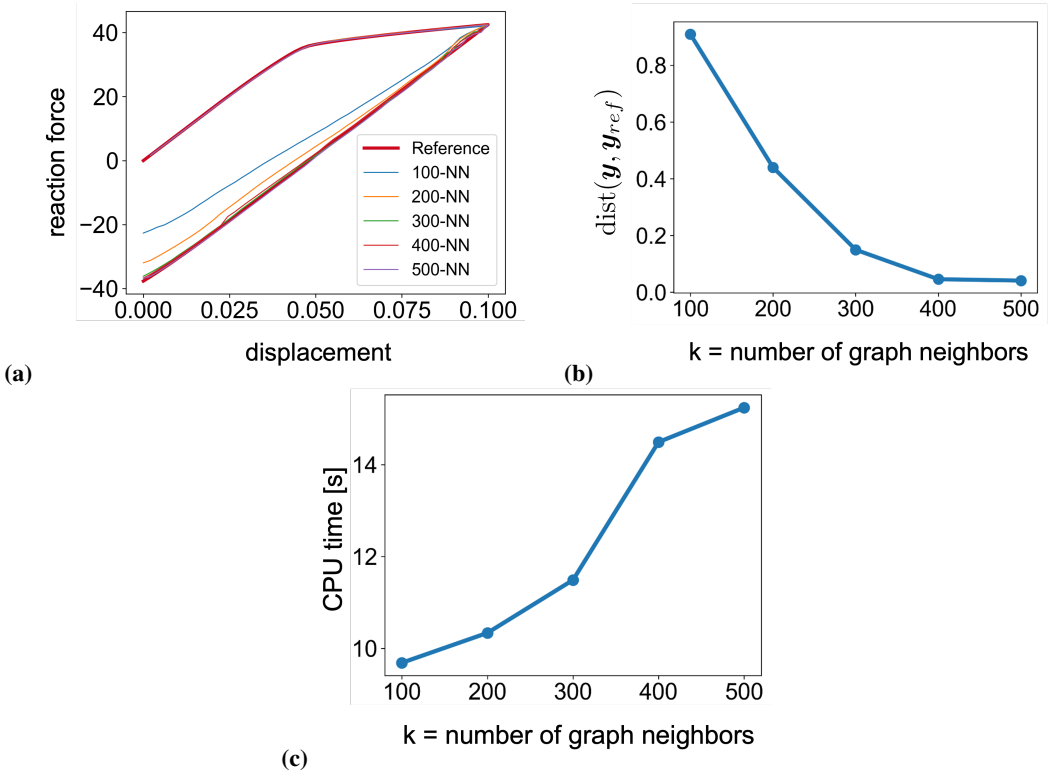

(a) **(b)**

(c)

Fig. 5: Influence of number of graph neighbors on accuracy and CPU time. a) displacement vs. reaction force. b) Distance (error) of the final load step. c) CPU times for different numbers of k using an user FE code.

neighbors. However, Fig. 5a) indicates, that the error is mainly introduced by the unloading point, which becomes critical for lower number of graph neighbors. The CPU times shown in Fig. 5 are obtained from computations on a 12-Core AMD Ryzen 9 3900X machine, using a self-developed user FE code for the projection operation. We note, that the CPU times using the ABAQUS interface are currently much higher due to additional interface costs. However, we conclude that the run-time with FE codes which has a dedicated interface is competitive in comparison to classical computations.

5 Conclusions

In this work, we have presented the data-driven computing paradigm with concepts for inelastic material behavior. We proposed the kNN-graph as an efficient search algorithm for data sets parametrized by the second law of thermodynamics. In addition, we proposed a history parametrization based on the mechanical work increment avoiding a rate-dependency. We presented a strategy to use commercial solver in a decoupled manner. Finally, we have demonstrated the proposed methods by a 2-d continuum example with plastic material behavior. Possible future works will cover sampling strategies for data acquisition with micro-mechanical models.

Acknowledgements All authors gratefully acknowledge the financial support of the Deutsche Forschungsgemeinschaft (DFG) and French Agence Nationale de la Recherche (ANR) through the project "Direct Data-Driven Computational Mechanics for Anelastic Material Behaviours" (ANR-19-CE46-0012-01, RE 1057/47-1, project number 431386925) within the French-German Collaboration for Joint Projects in Natural, Life and Engineering (NLE) Sciences. Open access funding enabled and organized by Projekt DEAL.

References

[1] T. Kirchdoerfer and M. Ortiz, Computer Methods in Applied Mechanics and Engineering **304**(June), 81–101 (2016).
[2] R. Eggersmann, L. Stainier, M. Ortiz, and S. Reese, Computer Methods in Applied Mechanics and Engineering **382**(August), 113855 (2021), arXiv: 2012.00357.
[3] Y. Kanno, Optimization Letters **13**(7), 1505–1514 (2019), arXiv: 1810.04394.
[4] L. T. K. Nguyen, R. C. Aydin, and C. J. Cyron, Computational Mechanics **70**(3), 621–638 (2022).
[5] R. Eggersmann, T. Kirchdoerfer, S. Reese, L. Stainier, and M. Ortiz, Computer Methods in Applied Mechanics and Engineering **350**(June), 81–99 (2019).
[6] K. Karapiperis, L. Stainier, M. Ortiz, and J. Andrade, Journal of the Mechanics and Physics of Solids **147**(February), 104239 (2021).

